New family of solitary waves in granular dimer chains with no precompression

K. R. Jayaprakash,* Yuli Starosvetsky,† and Alexander F. Vakakis‡
Department of Mechanical Science and Engineering, University of Illinois at Urbana Champaign, 1206 West Green Street, Urbana, Illinois 61822, USA
(Received 12 October 2010; revised manuscript received 26 January 2011; published 21 March 2011)

In the present paper we report the existence of a new family of solitary waves in general one-dimensional dimer chains with elastic interactions between beads obeying a strongly nonlinear Hertzian force law. These dimers consist of pairs of "heavy" and "light" beads with no precompression. The solitary waves reported herein can be considered as analogous to the solitary waves in general homogeneous granular chains studied by Nesterenko, in the sense that they do not involve separations between beads, but rather satisfy special symmetries or, equivalently antiresonances in their intrinsic dynamics. We conjecture that these solitary waves are the direct products of a countable infinity of antiresonances in the dimer. An interesting finding is that the solitary waves in the dimer propagate faster than solitary waves in the corresponding homogeneous granular chain obtained in the limit of no mass mismatch between beads (i.e., composed of only heavy beads). This finding, which might seem counterintuitive, indicates that under certain conditions nonlinear antiresonances can increase the speed of disturbance transmission in periodic granular media, through the generation of different ways for transferring energy to the far field of these media. From a practical point of view, this result can have interesting implications in applications where granular media are employed as shock transmitters or attenuators.

DOI: 10.1103/PhysRevE.83.036606 PACS number(s): 05.45.Yv, 45.70.−n, 46.40.−f

I. INTRODUCTION

Granular systems have been the subject of intense research interest for various reasons. They have potential applications in passive shock mitigation designs, condensed matter physics, and solid state physics. Granular systems are comprised of systems of discrete particles (beads) which may be similar (in monodisperse media) or dissimilar (in polydisperse media). One-dimensional granular systems have been well studied theoretically [1–3], numerically, and experimentally [1,4,5]. Moreover, it was shown that one-dimensional monodisperse systems support solitary waves which have attracted great interest and have been studied extensively [1–3]. Indeed, in homogeneous granular chains spatially localized waves may propagate without distortion due to counterbalancing of two effects, namely dispersion and strong nonlinearity due to Hertzian law interaction between beads. Such waves are denoted as *solitary waves*. One may rigorously define [6] a solitary wave propagating in a one-dimensional nonlinear medium as a right-traveling (left-traveling) localized disturbance whose transition from its asymptotic state at the limit $\xi = -\infty$ to its other asymptotic state at the limit $\xi = +\infty$ is localized in terms of the independent variable ξ, where $\xi = x - ct$ ($\xi = x + ct$), with x and t being spatial and temporal independent variables, respectively, and c the speed of the traveling wave.

Polydisperse systems typically exhibit waves that radiate energy to the far field as they travel, and thus distort their initial wave forms due to continuous energy "leakage." In the context of one-dimensional granular media much emphasis has been given to dimer systems [7–9], i.e., in systems composed of pairs of dissimilar beads. The dynamics of these systems have been studied both theoretically in the continuum approximation [4] and experimentally [4,8]. There has been little progress, however, in studying the dynamics of these systems analytically, taking into account the actual discrete nature of the bead interactions; perhaps this is due to the complexity of the nonlinear dynamical interactions occurring in these media, including the possibility of bead separation in the absence of precompression. Theocharis *et al.* [10] studied localized breathers in dimers under precompression taking into account the linear component in the dynamics that precompression introduces, but no similar results exist in the strongly nonlinear case dealt with here, in the absence of precompression.

In this work we focus on a particular feature of the dynamics of general one-dimensional elastic dimer chains with no precompression, and report the existence of a new family of perfectly localized solitary waves in these systems. As mentioned previously, this type of wave is not typical in polydisperse systems, such as the dimer chains consider herein. Solitary waves in dimers were observed and analyzed in Ref. [1] for large mass mismatch and in the limit of long wave approximation. The derived expression was a rescaled version of the expression for solitary waves in a homogeneous chain of similar beads derived in Ref. [1]. In our paper we denote this limiting system with large mass mismatch as "auxiliary system" and use the analytical expression derived in Ref. [2] as the $O(1)$ approximation in our asymptotic analysis. Furthermore, we consider higher-order approximations in the limit of small mass mismatch and show the existence of a class of solitary waves in the dimer. We show that this class of perfectly localized solitary waves (as defined above) is the direct result of special symmetries or antiresonances in the strongly (essentially) nonlinear dynamics of the uncompressed dimers. Moreover, we conjecture that there exists a countable infinity of members in this new family of solitary waves, corresponding to discrete values of a mass ratio parameter. This leads us to the interesting conjecture that nonlinear antiresonances may give rise to localized solitary waves in

*kalkunt1@illinois.edu
†staryuli@illinois.edu
‡avakakis@illinois.edu

a more general class of periodic polydisperse granular media, e.g., involving more complex spatial periodicities than the dimers considered in this work. An additional interesting feature of the reported family of solitary waves is that they propagate faster than the corresponding solitary waves in the homogeneous system obtained in the limit of no mass mismatch (i.e., in a homogeneous chain of identical beads). This observation very much applies to the normalized system under consideration in our work, and indicates that nonlinear antiresonances in granular media may speed up the propagation of disturbances within them. We present extensive numerical evidence of the presence of localized solitary waves in dimer chains with no precompression, and provide a general mathematical condition for the realization of this family of waves in these systems.

II. NUMERICAL EVIDENCE OF SOLITARY WAVES IN THE DIMER

We consider a one-dimensional dimer chain of spherical elastic beads in Hertzian contact with no precompression. Denoting the materials of two neighboring beads by the labels 1 and 2, and the displacement of the ith bead by u_i, the governing equations of motion are strongly nonlinear and given by

$$\begin{aligned} m_i \frac{d^2u_i}{dt^2} &= (4/3)E_*\sqrt{R}[(u_{i-1}-u_i)_+^{3/2} - (u_i - u_{i+1})_+^{3/2}], \\ m_{i+1}\frac{d^2u_{i+1}}{dt^2} &= (4/3)E_*\sqrt{R}[(u_i - u_{i+1})_+^{3/2} \\ &\quad - (u_{i+1}-u_{i+2})_+^{3/2}], \\ i &= \pm 1, \pm 3, \pm 5, \ldots, \end{aligned} \tag{1}$$

where $R_i = R_1$ and $R_{i+1} = R_2$; $m_i = m_1 = (4/3)\pi R_1^3\rho_1$ and $m_{i+1} = m_2 = (4/3)\pi R_2^3\rho_2$; and $E_* = E_1E_2/[E_2(1-\mu_1^2) + E_1(1-\mu_2^2)]$; E_1 (E_2) is the elastic modulus, R_1 (R_2) the radius, and μ_1 (μ_2) the Poisson's ratio of bead 1 (2). We note that the interaction force between neighboring beads is given by $F = (4/3)E_*\sqrt{R}\Delta^{3/2}$, where $R = R_1R_2/(R_1+R_2)$ and Δ is the relative displacement between neighboring beads. Moreover, the $(+)$ subscripts in Eq. (1) indicate that only the non-negative values of the terms in the parentheses should be considered and zero values should be assigned otherwise; this is due to the fact that in the absence of compressive elastic forces, neighboring beads separate. Note that in the absence of precompression the dynamics of the dimer is essentially nonlinear because the interacting forces between neighboring beads lack a linear component; as pointed out by Nesterenko [1] this class of systems constitutes a "sonic vacuum" as the speed of sound (defined by the linearized acoustics) is zero.

Introducing the nondimensionalizations,

$$x_i = \frac{u_i}{R_1}, \quad \tau = \left[\frac{E_*}{\pi R_1^2\rho_1}\left(\frac{R_2}{R_1+R_2}\right)^{1/2}\right]^{1/2} t, \tag{2}$$

we obtain the system of nondimensional equations,

$$\begin{aligned} \ddot{x}_i &= (x_{i-1}-x_i)_+^{3/2} - (x_i - x_{i+1})_+^{3/2}, \\ \varepsilon\ddot{x}_{i+1} &= (x_i - x_{i+1})_+^{3/2} - (x_{i+1}-x_{i+2})_+^{3/2}, \end{aligned} \tag{3a}$$

where the overdot denotes differentiation with respect to nondimensional time τ and the only nondimensional parameter is $\varepsilon = \rho_2R_2^3/\rho_1R_1^3$ scaling one of the pairs of beads of the dimer system (cf., Fig. 1). We note that if $R_1 = R_2$ the parameter ε is the ratio of the mass densities of the two materials of the dimer. In the following asymptotic analysis we will use ε as the small parameter of the problem by assuming that $0 < \varepsilon \ll 1$. Hence, we will be assuming that the dimer system is composed of "heavy" and "light" beads corresponding to normalized mass ratio equal to unity and ε, respectively. In the notation of the original system [Eq. (1)], bead 1 is the heavy bead and bead 2 is the light one. The clear advantage of studying the normalized dimer [Eq. (3a)] is that our results will have broad applicability to general dimer systems after appropriate rescaling. In addition to the asymptotic analysis we will explore numerically solitary waves realized for larger values of ε where the asymptotic analysis is not valid.

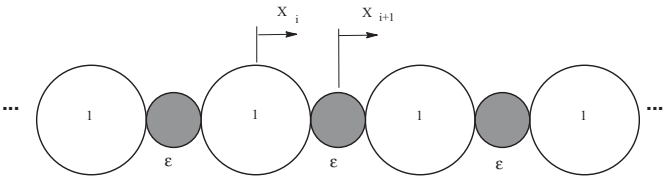

FIG. 1. Nondimensional dimer system composed of heavy and light beads.

We will show that the normalized dimer system [Eq. (3a)] has a special family of solitary waves (parametrized by energy) whose members are realized at a monotonically decreasing sequence of (discrete) values of ε. Because this dimer system is nonintegrable, asymptotic analysis of these solitary waves can be performed only in the limit of small ε, so initially we resort to direct numerical simulations to demonstrate their existence. For the numerical simulations we employ the setup shown in Fig. 2 and consider the parameter in the range $\varepsilon \in (0,1]$. In the system shown in Fig. 2 we apply an impulsive excitation equal to $F\delta(t)$ with $F = 2.7$ applied on the left-hand side of a dimer chain composed of a total of 251 beads. The right end of the chain has a fixed light bead (i.e., its center of mass is immovable) so that the nondimensionalization and rescaling employed in Eq. (3a) are valid. To demonstrate the existence of solitary waves in this system we consider a few pairs of beads in the middle of the chain and examine only primary pulse propagation, omitting reflections from the boundaries. Due to the inhomogeneity of the dimer system, intuitively one would expect a slow disintegration of the applied impulse, leading to small-amplitude oscillating "tails" in the corresponding responses of the light and heavy beads. This has been observed in previous experimental and numerical works (e.g., Ref. [11]). However, as shown in the following numerical simulations, at specific discrete values of ε (normalized mass ratio) the applied impulse gives rise to propagation of solitary waves which travel undeformed (i.e., their wave forms remain undistorted during

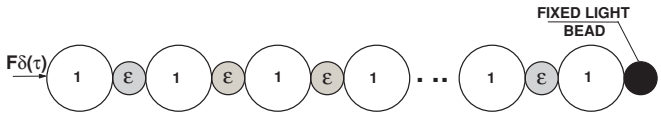

FIG. 2. Setup for numerical simulations.

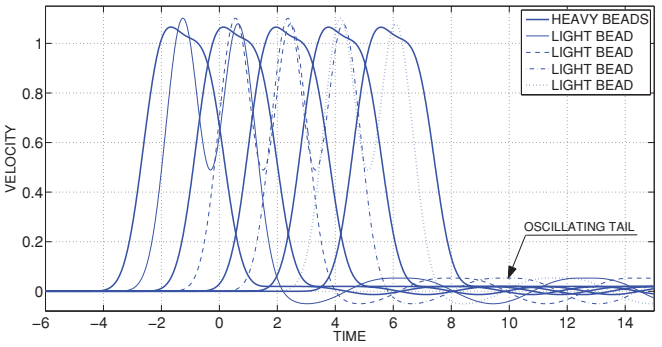

FIG. 3. (Color online) Velocity profiles of dimer pairs for $\varepsilon = 0.37$.

propagation) instead of disintegrating due to scattering at the interfaces between dissimilar beads.

In Fig. 3 we depict the velocities of four dimer pairs (beads 121–129 of the dimer) of the system of Fig. 2 for the arbitrary value of the mass ratio $\varepsilon = 0.37$. In this case we see that following the propagation of the main pulse, both the light and heavy beads of the dimer execute oscillations caused by residual energy left behind by the pulse, and appearing as oscillatory tails in the trail of the propagating pulse. Clearly, these tails are due to scattering of the main propagating pulse at the interfaces between beads. We note that this response is typical in the dynamics of the dimer, and demonstrates the (slow) disintegration of a propagating pulse. In fact, the oscillating tails are composed of *nonlinear traveling waves* that propagate behind the main pulse, and are similar to traveling waves in homogeneous granular chains studied in an earlier work [12]. The continuous radiation of traveling waves leads to a monotonic reduction of the amplitude of the main pulse as it propagates through the dimer.

Perhaps counterintuitively, at certain discrete values of the normalized mass ratio ε, localized solitary waves are formed in the dimer having the shape of traveling localized pulses with no residual oscillating tails left in their trails. Due to lack of energy radiation these solitary waves propagate unattenuated in the dimer and can be considered as analogs of the well-studied solitary pulse of the homogeneous granular chain [1]. In the case of the dimer, however, pulses with distinct wave forms are realized for the heavy and light beads. A similar observation of distinct propagating pulses in heavy and light beads in a dimer has been reported in [1]. These solitary waves are realized for a discrete set of values of the small parameter ε of the dimer, as demonstrated in the following section. Before we proceed with numerical evidence of the solitary waves in the dimer we comment on the two limiting configurations of the dimer system [Eq. (3a)], namely in the limits of the interval $0 < \varepsilon \leqslant 1$. In the lower limit $\varepsilon \to 0$ the dimer degenerates to a homogeneous chain with a normalized stiffness coefficient smaller than unity; this system will be designated as the "auxiliary system" [cf. Eq. (8b) below]. We note that the auxiliary system does not imply that there are gaps between heavy beads, but rather that the inertial effects of the light beads are negligible so that they act approximately as pure elastic springs. In the upper limit $\varepsilon \to 1$ the dimer degenerates again to a homogeneous chain with normalized stiffness coefficient

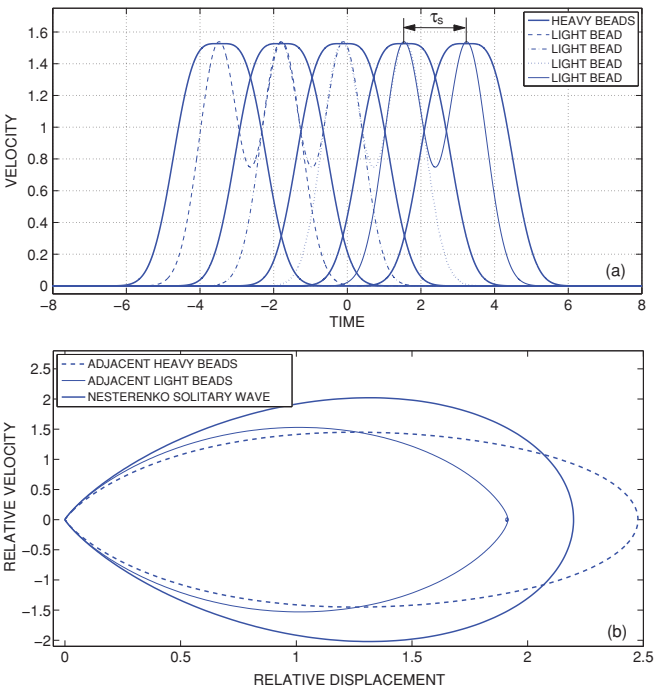

FIG. 4. (Color online) Solitary wave in the dimer with $\varepsilon \approx 0.3428$: (a) Velocity profiles of dimer pairs. (b) Phase plot of relative velocity versus relative displacement between successive heavy and light beads compared to the solitary wave of the homogeneous chain of heavy beads ($\varepsilon = 1$).

equal to unity; this is the homogeneous chain composed of only heavy beads.

In Fig. 4(a) we present the localized solitary wave realized in the dimer with $\varepsilon \approx 0.3428$. In this case there are no oscillating tails following the propagation of the main pulse. The velocity profiles of the heavy beads are in the form of a single hump and those of the light beads is a double hump (that is, a slow-scale single hump superimposed to fast-scale oscillations possessing significant amplitude). Although the heavy bead wave forms of these waves resemble the solitary wave discussed by Nesterenko [1], they have some very distinct differences. This is evidenced by the wave form of the heavy beads which is significantly affected by the fast-scale oscillations of the light beads, and also by the corresponding wave form of the light beads. However, in similarity to the Nesterenko solitary wave in the homogeneous chain, both velocity profiles of heavy and light beads decay to zero with increasing time and remain undistorted as the solitary wave propagates through the dimer. In Fig. 4(b) we depict both localized humps of the heavy and light beads in the phase plane (depicting relative velocity versus relative displacement for alternating heavy or light beads) and compare them to the solitary wave that develops in a homogeneous chain of heavy beads (obtained in the limit $\varepsilon \to 1$) with identical maximum displacement amplitude. It is clear that the two solitary humps of the dimer can be regarded as a disintegration of the solitary wave of the limiting homogeneous system due to scattering; yet, the fact that there is no disintegration of the main pulse to oscillatory tails implies that a special symmetry (or antiresonance) condition is realized at this special value

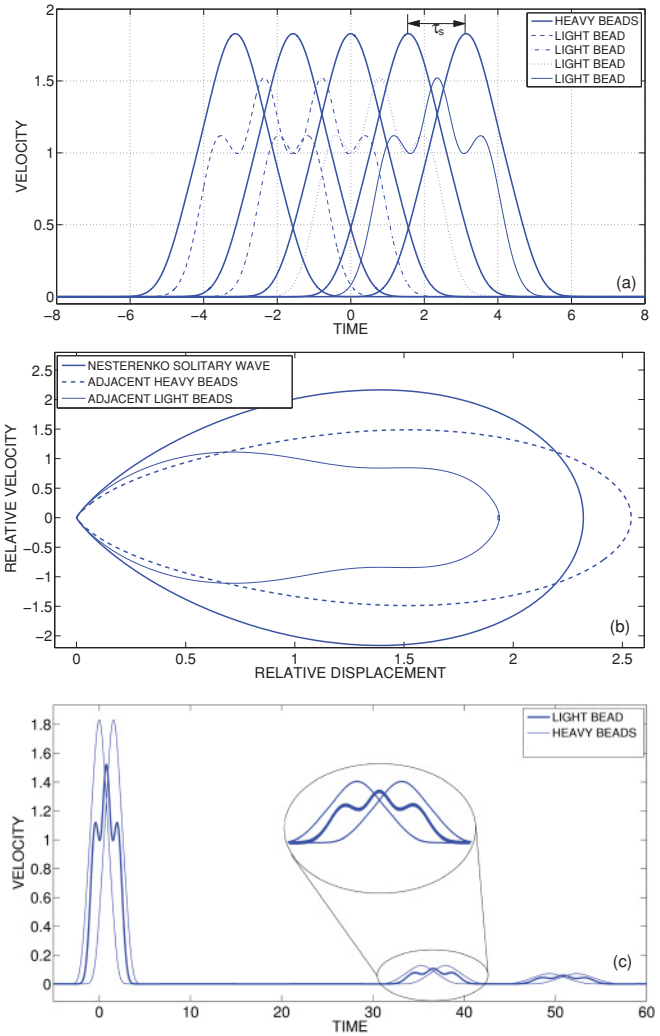

FIG. 5. (Color online) Solitary wave in the dimer with $\varepsilon \approx 0.1548$: (a) Velocity profiles of dimer pairs. (b) Phase plot of relative velocity versus relative displacement between successive heavy and light beads compared to the the solitary wave of the homogeneous chain of heavy beads ($\varepsilon = 1$). (c) Primary solitary wave followed by secondary solitary waves.

of ε preventing the complete disintegration of the pulse (as it occurs for arbitrary values of ε, cf. Fig. 3). Moreover, the addition of the alternating light beads in the dimer introduces a softening effect in the dynamics, and thus the amplitude of the solitary pulse between alternating heavy beads in the dimer is higher than that of the solitary wave in the corresponding homogeneous chain [see Fig. 4(b)].

Additional solitary waves realized in the dimer have been numerically detected for $\varepsilon \approx 0.1548$ (see Fig. 5), $\varepsilon \approx 0.0901$ (see Fig. 6), and $\varepsilon \approx 0.0615, 0.04537, 0.03448, 0.00868, \ldots$. Similar to the solitary wave for $\varepsilon \approx 0.3428$ these additional solitary waves have no oscillating tails but rather have velocity profiles that decay to zero with increasing time. With decreasing ε (i.e., increasing normalized mass mismatch) the light beads execute high-frequency oscillations while they are being compressed in between adjacent heavy beads; later we will denote this phase of the motion as the "squeeze mode."

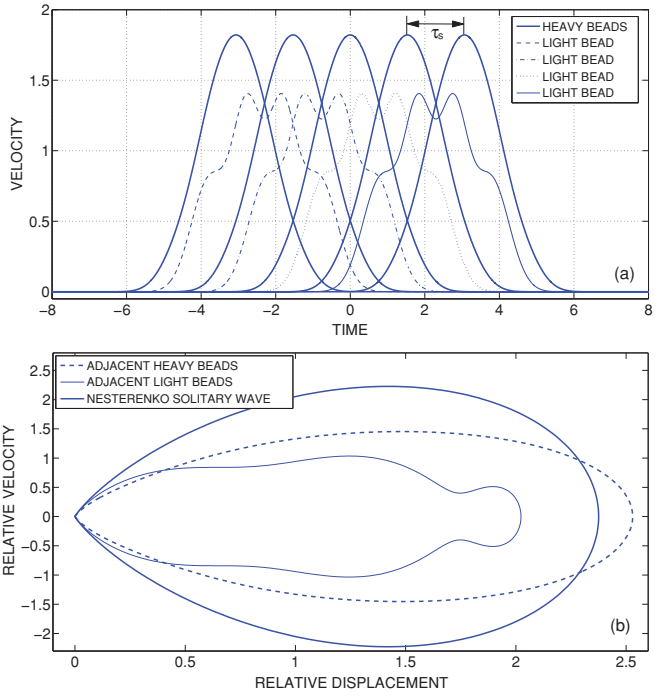

FIG. 6. (Color online) Solitary wave in the dimer with $\varepsilon \approx 0.0901$: (a) Velocity profiles of dimer pairs. (b) Phase plot of relative velocity versus relative displacement between successive heavy and light beads compared to the solitary wave of the homogeneous chain of heavy beads ($\varepsilon = 1$).

Generally, the frequency of oscillation of the light beads during the squeeze mode increases with decreasing ε. For a general value of ε, typically the light bead loses contact with its left neighboring heavy bead at the end of its compression phase (i.e., at the end of the squeeze mode), and retains a small portion (residual) of the energy of the propagating pulse. This generates a residual oscillation of the light bead even after the propagation of the primary pulse, which in turn leads to the formation of traveling waves in oscillating tails appearing at the wake of the propagation of the main pulse. These tails radiate energy to the far field in the opposite direction to that of the propagating pulse, and cause a continuous decrease of the amplitude (energy) of the primary pulse as it propagates through the dimer. Hence, for a typical value of ε no solitary wave can be formed.

In contrast, at the aforementioned discrete values of ε solitary waves are formed once the light beads stay in continuous contact with adjacent heavy beads (that is, no separation between light and heavy beads occurs), and the entire energy of the main pulse is conserved and transferred without loss from each heavy bead to the next heavy bead, after which each heavy bead reaches a stationary position at the end of the squeeze mode. As a result, no residual oscillating tails are formed in this case, there is no energy radiated to the far field, and the main pulse propagates unattenuated through the dimer. Clearly, this lossless transfer of energy through the dimer occurs only if certain symmetry conditions are satisfied. These conditions are formulated asymptotically in the next section where it is proved that a discrete set of solitary waves exists in the dimer accumulating to a definite limit as $\varepsilon \to 0$. It is

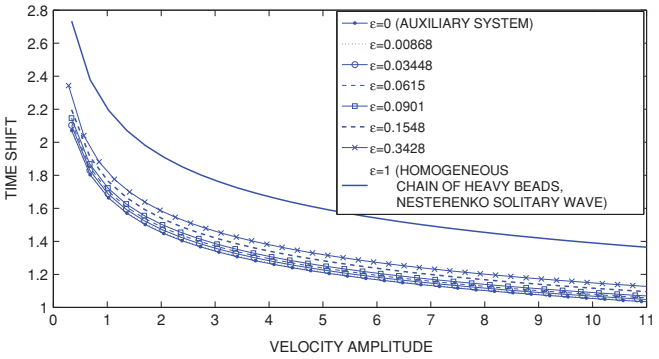

FIG. 7. (Color online) Time shifts τ_s versus peak velocities of the different families of solitary waves in the dimer.

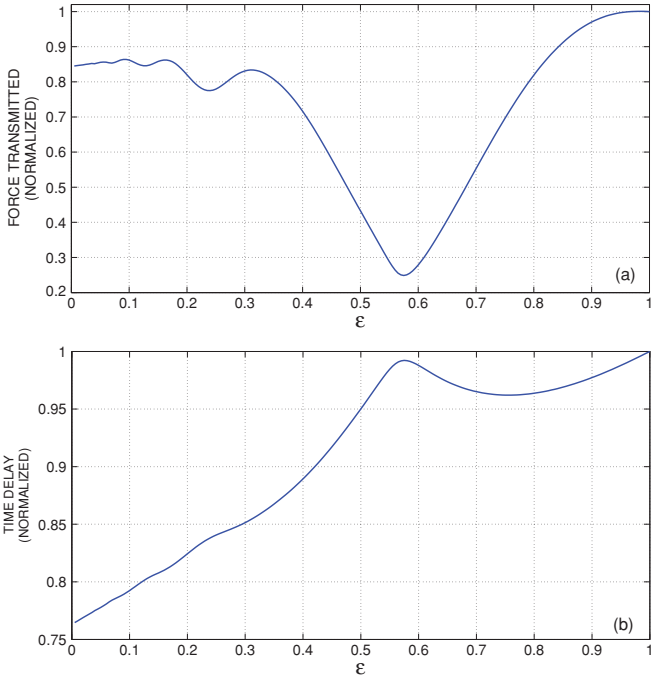

FIG. 8. (Color online) Normalized transmitted force (a) and normalized time delay (b) as functions of the normalized mass ratio parameter ε for an impulsively excited dimer.

also important to point out the formation of secondary solitary waves [cf. Fig. 5(c)] belonging to the same class of solitary waves discussed so far. These secondary waves are generated due to separations of the initial beads of the system following the application of the impulse, and the fact that they have the exact form of the solitary wave provides additional numerical evidence that at the mentioned discrete values of ε the solitary waves provide the principal (fundamental) mechanism for transferring energy in the dimer. We conclude that this family of solitary waves constitutes the most natural type of localized, traveling pulses in the dimer system for the mentioned special discrete values of ε, in similarity to the solitary waves studied by Nesterenko [1], which provide the principal mechanism for transferring energy in homogeneous granular chains.

A particularly interesting feature of solitary waves in the dimer chain is that their phase velocities are higher than the phase velocity of the solitary wave in the homogeneous system obtained in the limit $\varepsilon \to 1$; in fact the solitary waves become faster as the normalized mass ratio ε decreases. Indeed, in Fig. 7 we depict the time shift [labeled as τ_s in Figs. 4(a), 5(a), and 6(a)] of a solitary wave in the dimer (defined as the time difference between velocity peaks of successive heavy beads) plotted against the velocity amplitude of the solitary wave. In essence, this plot represents the energy–speed relations for the different families of solitary waves in the dimer. Due to the discrete nature of the system, defining phase velocity as in continuum systems is not possible. An analogous quantity, which can be attributed to the velocity of propagation of the solitary waves, is the time shift that we present in Fig. 7. The lower bounding curve corresponds to the auxiliary system obtained in the limit $\varepsilon \to 0$, and corresponds to the fastest class of solitary waves. As shown in the asymptotic analysis that follows, every point in the lower bounding curve represents an accumulation point of solitary waves as $\varepsilon \to 0$ (that is, fixing the peak velocity amplitude of the solitary wave and letting $\varepsilon \to 0$). Moreover, there is an upper bounding curve corresponding to the solitary wave of the homogeneous chain corresponding to $\varepsilon = 1$, which demonstrates that every solitary wave propagating in the dimer is faster than the solitary wave propagating in the corresponding homogeneous system composed exclusively of heavy beads. We also note that due to the homogeneous nonlinear potential of the Hertzian law interaction [13], the dimer system is fully re-scalable in the sense that for any input impulse the time shifts for the solitary waves bear a constant ratio compared to that of the solitary wave realized in the limiting homogeneous chain with $\varepsilon = 1$.

To demonstrate the effect that the solitary waves can have on the response of the dimer chain to shock excitations we reconsider the system of Fig. 2 with a total of 85 heavy and light beads, with the last heavy bead of the dimer being in contact with a fixed light bead. Again, no precompression in the chain exists. A unit impulse excitation is applied to the first bead on the left end of the dimer chain. As described previously this system is fully rescalable, and thus, for any applied impulse the ratio of the force F_t transmitted to the fixed light bead over the corresponding force in the limiting homogeneous chain with $\varepsilon = 1$ is constant for any value of ε. This argument is valid also for the time delay τ_d between the application of the pulse on the first bead at the left end of the dimer chain (Fig. 2) and its arrival to the right fixed bead. It follows that we only need to consider the dynamics of the dimer subject to a unit impulse, with our results being valid at different energies (or applied pulses). Again, this result originates from the "homogeneous" nature of the nonlinear interaction potential between beads, leading to dynamics that are fully rescalable with energy.

In Fig. 8(a) we depict the force transmitted to the fixed light bead normalized with respect to the corresponding force transmitted in the homogeneous system with $\varepsilon = 1$. From these results it is clear that the force transmitted is always smaller for the case of the dimer compared to the homogenous chain. The intermediate local peaks of normalized transmitted force (occurring at $\varepsilon \approx 0.3428, 0.1548, 0.0901, \ldots$) are realized at the specific values of ε for which solitary waves are formed, because only then energy is transferred unattenuated through the dimer. On the contrary, in between the local

peaks of normalized transmitted force where no solitary waves are formed and the propagating pulse disintegrates due to scattering at bead interfaces, the normalized transmitted force decreases, with maximum reduction of the order of 75% of the normalized transmitted force occurring for $\varepsilon \approx 0.59$. These results indicate that the solitary waves represent an efficient mechanism for transferring energy through the dimer system. The normalized time delay [14] (with respect to the corresponding time delay for the homogeneous system with $\varepsilon = 1$) for the dimer is presented in Fig. 8(b), from which we infer that for an arbitrary value $0 < \varepsilon < 1$ the normalized time delay is smaller than unity. This leads us to the claim that solitary waves in the dimer propagate faster than the Nesterenko solitary wave in the homogeneous system of heavy beads. It is worth noting that the number of beads and the loading conditions are identical for each dimer system considered in Fig. 8(b), and we vary only the normalized mass ε. Clearly, the time delay described here is more applicable for practical and/or experimental applications instead of theoretical analysis because it does not provide a rigorous measure of the speed of the solitary wave in the dimer. From a theoretical perspective, the time shift (Fig. 7) is a valid measure to describe the speed of solitary waves and Fig. 7 rigorously evidences our claim of faster propagation of solitary waves in a dimer when compared to that in a homogeneous chain of heavy beads. Moreover, the previous observations are valid only for the normalized system under consideration, wherein the mass of the heavy bead is fixed to unity, and only the normalized mass of the light bead is varied in the range $\varepsilon \in (0\,1]$.

The previous numerical results show that a granular chain with periodic inhomogeneities can support different classes of solitary waves. The solitary waves with perfect localization (i.e., with no oscillating tails following the propagation of the main pulse) considered here differ from traveling waves observed by previous researchers [8,11] in these systems that can at best be described as either quasistationary primary pulses or solitary-like pulses, but are not solitary waves following the definition in Ref. [6]. In the context of our discussion the propagating solitary waves conserve their energy, do not radiate energy to the far field and retain their wave forms intact.

In the family of solitary waves considered herein, even though the light beads execute relatively high-frequency oscillations (in their squeeze mode) they do not lose contact with their neighboring heavy beads even towards the end of the squeeze mode. Such behavior can occur under special conditions, that is, only if the velocity (displacement) wave form of each light bead possesses special symmetric (antisymmetric) properties. For the velocity wave form to be symmetric a light bead should end its high-frequency oscillation with precisely *zero velocity*, i.e., with precisely the initial velocity with which it begins its motion during the squeeze mode. Such synchronization between the motion of the light and heavy beads can only imply that a certain *resonance or antiresonance condition* is satisfied when a solitary wave is formed; this will be confirmed in the theoretical study of the next section. For smaller values of ε (i.e., for large mass mismatch in the dimer) the oscillation of the light bead does not affect the motion of its neighboring heavy beads. It follows that in the limit of small ε we may introduce multiple time scales to describe the dynamics of the solitary waves: a *fast time scale* that governs the relatively high-frequency oscillations of the light beads, and a *slow time scale* that governs the slowly varying localized pulse in the heavy beads. However, as the normalized mass ratio increases and we progress towards the region of upper bound ($\varepsilon \approx 0.3428$) of realization of these solitary waves, we clearly see that the amplitude of oscillations of the light beads become comparable to the solitary pulse in the heavy beads. At this stage the time scale separation breaks down and we may no longer partition the dynamics of the heavy and light beads in terms of slow and fast components (that is, the time scales become entangled). Hence, the normalized mass ratio $\varepsilon \approx 0.3428$ represents an upper bound for the existence of solitary waves in the dimer, in the sense that beyond this point no solitary waves can be formed, with the exception, of course, of the well-studied solitary wave in the limiting homogeneous system with $\varepsilon = 1$ studied by Nesterenko [1].

The fact that the solitary waves in the dimer propagate faster than the solitary wave in the limiting system with $\varepsilon = 1$ might seem counterintuitive. Taking into account, however, that solitary waves in the dimer are formed under conditions of antiresonance, it implies that antiresonance phenomena may be responsible for the higher phase velocities of the solitary waves in the dimer. As shown in the numerical results of Fig. 8 the existence of solitary waves in granular chains with periodicity facilitates the transmission of energy and increases the speed of disturbance transmission in these media. This implies that antiresonance phenomena in granular chains represent an important dynamical mechanism which significantly affects the capacity of these media to transmit disturbances.

In the next section we perform a theoretical study of the dimer system in the limit of small ε in order to confirm the numerical results of this section, and to study the resonance conditions that lead to the formation of solitary waves in the dimer for specific values of normalized mass ratio ε.

III. THEORETICAL STUDY

Considering again the nondimensional governing equations for the dimer,

$$\begin{aligned} \ddot{x}_i &= (x_{i-1} - x_i)_+^{3/2} - (x_i - x_{i+1})_+^{3/2}, \\ \varepsilon \ddot{x}_{i+1} &= (x_i - x_{i+1})_+^{3/2} - (x_{i+1} - x_{i+2})_+^{3/2}, \\ i &= \pm 1, \pm 3, \pm 5, \ldots, \end{aligned} \tag{3b}$$

we assume that $0 < \varepsilon \ll 1$, i.e., study the dynamics in the limit of large normalized mass mismatch. The index notation in Eq. (3b) indicates that odd indices correspond to heavy beads, and even indices to light beads. The subscripts (+) will be dropped from here on as we will be concerned only with primary pulse transmission in the dimer, that is, we will be concerned only with the phase of the squeeze mode during which the light beads are under continuous compression from their neighboring heavy beads so that no separation between beads occurs.

Clearly, for sufficiently small values of ε, system (3b) is in the form of a singularly perturbed problem that calls for a slow-fast time scale separation. We will be interested only in primary pulse transmission in the dimer, omitting secondary waves.

Within this context we may study solitary wave transmission in the dimer because this corresponds exclusively to primary pulse transmission with no separation between beads. Hence, we describe the dynamics of solitary wave formation by introducing the following asymptotic approximation for the bead displacements of the dimer:

$$\begin{aligned} x_i &= x_{i0}(t_0) + \varepsilon^{\alpha} x_{i1}(t_1) + \cdots \text{ (heavybeads)}, \\ x_{i+1} &= x_{(i+1)0}(t_0) + \varepsilon^{\gamma} x_{(i+1)1}(t_1) + \cdots \text{ (lightbeads)}, \end{aligned} \tag{4}$$

where t_0 and t_1 are distinct time scales of the dynamics defined as follows:

$$t_0 = \tau, \;\; t_1 = \varepsilon^{\beta} t_0, \tag{5}$$

and the real exponents α, β, γ are to be determined by balancing terms at various orders of approximation of the asymptotic analysis. Substituting Eqs. (4) and (5) into Eq. (3b), and expanding the rational powers in a power series with respect to ε we obtain the following set of governing equations valid in the limit of sufficiently small ε:

$$\begin{aligned} \ddot{x}_{i0} + \varepsilon^{\alpha+2\beta} x_{i1}'' &= (x_{(i-1)0} - x_{i0})^{3/2} - (x_{i0} - x_{(i+1)0})^{3/2} \\ &\quad + (3/2)(x_{(i-1)0} - x_{i0})^{1/2}(\varepsilon^{\gamma} x_{(i-1)1} - \varepsilon^{\alpha} x_{i1}) \\ &\quad - (3/2)(x_{i0} - x_{(i+1)0})^{1/2}(\varepsilon^{\alpha} x_{i1} - \varepsilon^{\gamma} x_{(i+1)1}) \\ &\quad + O(\|\varepsilon^{\alpha} x_{i1} - \varepsilon^{\gamma} x_{(i+1)1}\|^2), \end{aligned} \tag{6}$$

$$\begin{aligned} &\varepsilon(\ddot{x}_{(i+1)0} + \varepsilon^{\gamma+2\beta} x_{(i+1)0}'') \\ &\quad = (x_{i0} - x_{(i+1)0})^{3/2} - (x_{(i+1)0} - x_{(i+2)0})^{3/2} \\ &\qquad + (3/2)(x_{i0} - x_{(i+1)0})^{1/2}(\varepsilon^{\alpha} x_{i1} - \varepsilon^{\gamma} x_{(i+1)1}) \\ &\qquad - (3/2)(x_{(i+1)0} - x_{(i+2)0})^{1/2}(\varepsilon^{\gamma} x_{(i+1)1} - \varepsilon^{\alpha} x_{(i+2)1}) \\ &\qquad + O(\|\varepsilon^{\alpha} x_{i1} - \varepsilon^{\gamma} x_{(i+1)1}\|^2). \end{aligned} \tag{7}$$

In the equations above overdots indicate differentiation with respect to the time scale $t_0 = \tau$ and primes represent differentiation with respect to the time scale t_1. By considering the order of magnitude of the various terms in Eqs. (6) and (7), the exponents in the asymptotic analysis are chosen as $\alpha = 2$, $\beta = -1/2$, and $\gamma = 1$ because this leads to appropriate balancing of terms at successive orders of approximation. It follows that $t_0 = \tau$ is the slow time scale, whereas $t_1 = \varepsilon^{-1/2}\tau$ the fast time scale of the dynamics.

Considering the zeroth-order approximation in Eqs. (6) and (7), respectively, we obtain the following set of equations that govern the *slow dynamics* of the dimer:

$$\begin{aligned} \ddot{x}_{i0} &= (x_{(i-1)0} - x_{i0})^{3/2} - (x_{i0} - x_{(i+1)0})^{3/2}, \\ x_{(i+1)0} &= \frac{x_{i0} + x_{(i+2)0}}{2}. \end{aligned} \tag{8a}$$

The first set of nonlinear ordinary differential equations in Eq. (8a) provides the first-order approximation of the dynamics of the heavy beads, whereas the second set of linear algebraic equations provides the first-order approximation of the dynamics of the light beads. It is clear that system (8a) is expressed exclusively in terms of the slow time scale t_0, so the leading-order approximations of the responses of both the heavy and light mass beads of the dimer are slow dynamical motions.

By simple algebraic manipulations, Eq. (8a) may be rewritten in the following form:

$$\begin{aligned} \ddot{x}_{i0} &= (1/2)^{3/2}[(x_{(i-2)0} - x_{i0})^{3/2} - (x_{i0} - x_{(i+2)0})^{3/2}], \\ x_{(i+1)0} &= \frac{x_{i0} + x_{(i+2)0}}{2}. \end{aligned} \tag{8b}$$

It follows that the first-order approximation of the (slowly varying) motion of the heavy beads is identical to the response of a homogeneous granular chain [i.e., the first set of nonlinear ordinary differential equations in Eq. (8b), which is in terms only of the responses of the heavy beads], whereas the first-order approximation of the response of the light beads is expressed in terms of the (slowly varying) responses of the heavy beads [i.e., the second set of linear algebraic relations in Eq. (8b)]. In fact the homogeneous granular chain in Eq. (8b) corresponds to the auxiliary system defined in the previous section derived in the limit $\varepsilon \to 0$ of the dimer.

Hence, in the first-order of approximation the slow dynamics of the light beads is determined in terms of the slow dynamics of the heavy beads. At this point we emphasize that we are interested only in the analytical description of the primary pulse propagating in the dimer. Therefore, we select the solution of the first set of equations in Eq. (8b) to be the solitary wave of the homogenous system for which analytical approximations have been derived in the literature [1,2,12]. Following Ref. [2] the analytical approximation of the slowly varying motion of the heavy beads is expressed as

$$x_{i0}(t_0) = S_i(\kappa t_0), \quad \kappa = (1/2)^{3/4}, \tag{9a}$$

where

$$\begin{aligned} S_i(\kappa t_0) &= S[\kappa(t_0 - iT)], \\ S(\xi) &= A + (A/2)(\tanh\{[C_1(\xi/T) \\ &\quad + C_3(\xi/T)^3 + C_5(\xi/T)^5]/2\} - 1), \\ C_1 &= 2.395\,36, \quad C_3 = 0.268\,529, \quad C_5 = 0.006\,134\,7. \end{aligned} \tag{9b}$$

In Eq. (9b) A is the amplitude of the solitary wave and T is the time shift in the response between the maxima of two successive heavy beads (or the peak-peak delay for velocity pulse transmission between successive heavy beads). Accordingly, the slowly varying component of the motion of the light beads is expressed as

$$x_{(i+1)0}(t_0) \equiv s_{(i+1)}(\kappa t_0) = \frac{S_i(\kappa t_0) + S_{i+2}(\kappa t_0)}{2}. \tag{9c}$$

Thus we observe that the $O(1)$ approximation of the responses of both the heavy and light beads always decays to zero. Such an approximation is valid only in the limit of very small ε. Such a solution was previously derived by employing the long wave approximation by Nesterenko [1]. This long wave approximation and the solitary wave approximation used in our work are compared in Ref. [15]. Although such approximations well predict the dynamics of the heavy beads for smaller ε, the responses of the light beads need not necessarily decay to zero for arbitrary values of ε. It follows that in order to realize solitary waves we need to find the discrete values of ε for which higher-order asymptotic corrections of the dynamics of the light bead decay to zero.

Proceeding to the next order approximation, at $O(\varepsilon)$ we derive the following equations governing the *fast dynamics* of the heavy and light beads:

$$x''_{i1}(t_1) = (3/2)[S_{(i-1)}(\kappa t_0) - S_i(\kappa t_0)]^{1/2} x_{(i-1)1}(t_1) + (3/2)[S_i(\kappa t_0) - S_{(i+1)}(\kappa t_0)]^{1/2} x_{(i+1)1}(t_1),$$

$$x''_{(i+1)1}(t_1) + \Omega^2_{i+1}(t_0) x_{(i+1)1}(t_1) = f_{i+1}(t_0), \qquad (10)$$

where

$$\Omega^2_{i+1}(t_0) = 3\left[\frac{S_i(\kappa t_0) - S_{(i+2)}(\kappa t_0)}{2}\right]^{1/2},$$
$$f_{i+1}(t_0) = -\ddot{s}_{(i+1)}(\kappa t_0)$$

are the square of a slowly varying natural frequency and the slow varying excitation, respectively. These equations provide the leading-order approximation to the fast dynamics of the dimer for solitary wave propagation. We note that the second set of Eqs. (10) is uncoupled from the first set and governs the fast oscillations of the light beads. It is interesting to point out that this is in the form of uncoupled linear oscillators with slowly varying frequencies and excitations. Once analytical approximations for the fast oscillations of these oscillators are derived, the fast oscillations of the heavy beads can be approximated by integrating twice the first set of Eqs. (10). Hence, it is interesting to note that in the next order of approximation of the solitary wave solution the fast dynamics of the heavy beads is determined in terms of the fast dynamics of the light beads, which is the reverse of what occurred in the slow dynamics at the leading order of approximation.

From the previous discussion it is clear that we only need to focus on the second set of slowly varying linear oscillators [Eq. (10)] because these determine completely the fast dynamics of the dimer for solitary wave propagation. Once an analytical approximation of the fast oscillation of an arbitrary light bead, say the $2p$th light bead, $p \in Z$, is computed, the responses of the other light beads can be determined by imposing appropriate time shifts (i.e., multiples of T) to the solution. Hence, in the remainder of this section we focus exclusively on the analysis of the following linear oscillator with slowly varying frequency and forcing:

$$x''_{(2p)1}(t_1) + \Omega^2_{2p}(t_0) x_{(2p)1}(t_1) = f_{2p}(t_0), \qquad (11)$$

which governs the fast oscillation of the $2p$th light bead of the dimer for solitary wave propagation. Clearly, localized solutions in terms of the slow time scale of Eq. (11) correspond to solitary waves in the dimer through appropriate time shifts.

Before we proceed to the analytic approximations of the localized solutions of Eq. (11), we discuss the symmetry conditions that these solutions should satisfy according to the numerical results of the previous section. From the velocity profiles of the three localized solitary waves depicted in Figs. 4, 5, and 6 we notice that they have reflectional symmetry with respect to the time instant where the two neighboring heavy beads attain equal (but nonzero) velocities. Based on this observation we formulate a *symmetry condition* for the solitary waves of the dimer. Indeed, for the $(i+1)$th light bead a reference time instant $\tau = T_{s(i+1)}$ is defined as the time instant at which its velocity profile attains a local extreme and the ith and $(i+2)$th neighboring heavy beads [which compress the $(i+1)$th light bead in the squeeze mode] attain identical but nonzero velocities. The symmetry condition states that the velocity profile of the $(i+1)$th light bead has reflectional symmetry with respect to the reference time instant $\tau = T_{s(i+1)}$. In fact this time instant may also be regarded as the point of maximum compression of the light bead by its neighboring heavy beads. Therefore, for the velocity profile v_{i+1} of the $(i+1)$th light bead we formulate the following symmetry condition:

$$v_{i+1}(T_{s(i+1)} - u) = v_{i+1}(T_{s(i+1)} + u), \ \forall\, u \in R,$$
$$v_i(T_{s(i+1)}) = v_{i+2}(T_{s(i+1)}), \ \ i = \pm 1, \pm 3, \pm 5, \ldots. \qquad (12)$$

Note that if the symmetry condition (12) is satisfied, it automatically prevents the appearance of an oscillatory tail in the velocity profile of the light intruder (as in Fig. 3) resulting from secondary reflections in the trail of the propagation of the primary pulse. Hence, the symmetry condition (12) provides the necessary condition for the formation of a localized solitary wave in the dimer by preventing scattering of the main pulse at the interfaces between beads.

The symmetry condition for the velocity profile of the $(i+1)$th light bead implies that the corresponding displacement profile is *antisymmetric* with respect to the reference time instant $\tau = T_{s(i+1)}$. Recalling that the asymptotic approximation of the response of the light bead is given by

$$x_{i+1}(t_0, t_1, \ldots) = s_{i+1}(\kappa t_0) + \varepsilon x_{(i+1)1}(t_1) + \cdots,$$
$$t_0 = \tau, \ \ t_1 = \varepsilon^{-1/2}\tau,$$

and that the slow part $s_{i+1}(\kappa t_0)$ is already antisymmetric with respect to the reference time instant, condition (12) implies that the fast part of the dynamics, $x_{(i+1)1}(t_1)$, should also be antisymmetric with respect to the reference time instant. It follows that a necessary condition for the existence of the solitary wave in the dimer is that the fast dynamics [Eq. (11)] of the $(i+1)$th light bead is antisymmetric with respect to the reference time instant.

Returning to the fast dynamics [Eq. (11)] of the $2p$th light bead, without loss of generality we assume that its reference time instant is equal to zero, i.e., $T_s(2p) = 0$. We recognize that by construction the excitation $f_{2p}(t_0)$ is antisymmetric, and the natural frequency squared $\Omega^2_{2p}(t_0)$ is symmetric with respect to the reference time instant $\tau = 0$. It follows that in order to satisfy the antisymmetry condition of the fast dynamics [Eq. (11)] with respect to $\tau = 0$ we require that

$$x_{(2p)1}(t_1 = 0) = 0. \qquad (13)$$

This provides a *necessary condition* for the formation of the solitary wave in the dimer.

A second condition that we need to impose on the asymptotic solution of the $2p$th light bead is that it is localized in time and decays as $\tau \to \pm\infty$. Recalling the asymptotic approximation of the dynamics of the light bead, $x_{2p}(t_0, t_1, \ldots) = s_{2p}(\kappa t_0) + \varepsilon x_{(2p)1}(t_1) + \cdots$, and taking into account that the slow part of the dynamics already satisfies this asymptotic requirement in the far field, we impose the condition that $\lim_{t_1 \to \pm\infty} x'_{(2p)1}(t_1) = 0$. Taking into account

the antisymmetry condition for the fast dynamics it suffices to impose the condition

$$\lim_{t_1\to+\infty} x'_{(2p)1}(t_1) = 0. \tag{14}$$

The combined relations (13) and (14) formulate *necessary and sufficient conditions* for the formation of solitary waves in the dimer and provide the appropriate boundary conditions for the asymptotic approximation of the fast dynamics of the $2p$th light bead.

Our next goal is to find the discrete values of ε for which conditions (13) and (14) are satisfied. Recalling that a small parameter ε enters into the problem [Eq. (11)] through the differentiation with respect to the fast time scale, it is convenient to rewrite Eq. (11) in terms of the slow time scale $t_0 = \tau$ as follows:

$$\ddot{x}_{(2p)1}(\tau) + \frac{\Omega_{2p}^2(\tau)}{\varepsilon} x_{(2p)1}(\tau) = \frac{f_{2p}(\tau)}{\varepsilon}, \tag{15}$$

and seek the initial conditions $x_{(2p)1}(0) = 0$, $\dot{x}_{(2p)1}(0) = V$ and the specific values of ε for Eq. (14) to be satisfied. This task was performed numerically and the discrete set of values $\{\varepsilon_n\}$ and initial velocities $\{V_n\}$ required for the formation of solitary waves in the dimer were computed.

Before we review the numerical solutions of this problem, however, we explore the possibility of constructing analytical approximations of the solitary solutions of Eq. (15). To this end we apply the Wentzel-Kramers-Brillouin (WKB) approximation [16] under the assumption of ε being sufficiently small. It is well known that the WKB approach ceases to be valid in the vicinity of turning points (i.e., at points of nullification) of $\Omega_{2p}(\tau)$, and in our case we are interested to find an approximation of the solutions of Eq. (15) in the semi-infinite time interval $\tau \in [0, +\infty)$. However, $\Omega_{2p}(\tau)$ is an exponentially decaying function of time so there exists a turning point at infinity. It follows that for relatively small values of $\Omega_{2p}(\tau)$ the proposed methodology may become invalid. According to the WKB approximation [16] we seek the solution of Eq. (15) subject to the aforementioned initial conditions in the form

$$x_{(2p)1}(\tau) \sim \exp\left[\frac{1}{\varepsilon^{1/2}} \sum_{n=0}^{\infty} \varepsilon^{n/2} G_n(\tau)\right] + \frac{f(\tau)}{\Omega_{2p}(\tau)^2}, \quad \varepsilon \to 0, \tag{16}$$

where the first term represents the homogeneous solution of Eq. (15), whereas the second term is a particular solution of the problem. Although this approximation is valid in a finite interval $\tau \in [0, T^*]$, $T^* < +\infty$, as shown below this interval provides the main contribution to the sought solitary wave. Inserting Eq. (16) into Eq. (15), and considering the main (zeroth-order) terms we obtain the following results [where $j = (-1)^{1/2}$]:

$$\begin{aligned} G_0(\tau) &= \pm j \int_0^\tau \Omega_{2p}(\zeta) d\zeta \Rightarrow \\ x_{(2p)1}(\tau) &\cong \frac{C_1}{\sqrt{\Omega_{2p}}} \exp\left[\frac{j}{\sqrt{\varepsilon}} \int_0^\tau \Omega_{2p}(\zeta) d\zeta\right] \\ &\quad + \frac{C_2}{\sqrt{\Omega_{2p}}} \exp\left[\frac{-j}{\sqrt{\varepsilon}} \int_0^\tau \Omega_{2p}(\zeta) d\zeta\right] + \frac{f(\tau)}{\Omega_{2p}(\tau)^2} \end{aligned}$$

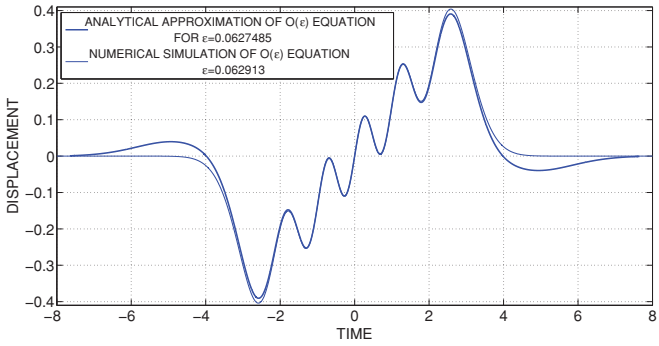

FIG. 9. (Color online) Comparison of the numerical solution of the fast dynamics [Eq. (11)] and the WKB analytical approximation (19).

$$\begin{aligned} &\equiv \frac{\tilde{C}_1}{\sqrt{\Omega_{2p}}} \cos\left[\frac{1}{\sqrt{\varepsilon}} \int_0^\tau \Omega_{2p}(\zeta) d\zeta\right] \\ &\quad + \frac{\tilde{C}_2}{\sqrt{\Omega_{2p}}} \sin\left[\frac{1}{\sqrt{\varepsilon}} \int_0^\tau \Omega_{2p}(\zeta) d\zeta\right] + \frac{f(\tau)}{\Omega_{2p}(\tau)^2}, \\ &\varepsilon \to 0. \end{aligned} \tag{17}$$

The antisymmetry condition $x_{(2p)1}(0) = 0$ yields $\tilde{C}_1 = 0$. Imposing the second initial condition $\dot{x}_{(2p)1}(0) = V$ we determine the second constant $\tilde{C}_2$ as follows:

$$\tilde{C}_2(\varepsilon, V) = \left[\frac{\varepsilon}{\Omega(0)}\right]^{1/2} \left[V - \frac{\dot{f}(0)}{\Omega^2(0)}\right], \tag{18}$$

where it holds that $\dot{\Omega}_{2p}(0) = 0, \dot{f}(0) \neq 0$, owing to the symmetric and antisymmetric nature of these functions, respectively. Therefore, the WKB asymptotical approximation in the finite interval $\tau \in [0, T^*]$ reads

$$\begin{aligned} x_{(2p)1}(\tau) &\cong \frac{\tilde{C}_2(\varepsilon, V_0)}{\sqrt{\Omega_{2p}}} \sin\left[\frac{1}{\sqrt{\varepsilon}} \int_0^\tau \Omega_{2p}(\zeta) d\zeta\right] + \frac{f(\tau)}{\Omega_{2p}(\tau)^2}, \\ &\varepsilon \to 0. \end{aligned} \tag{19}$$

Although the limiting condition (14) in the far field cannot be imposed in the WKB approximation (because as mentioned previously the problem has a turning point at $\tau \to +\infty$), nevertheless we can find sets of values $\{\varepsilon_n, V_n\}$ for which the condition $\lim_{\tau\to+\infty} \dot{x}_{(2p)1}(\tau) = 0$ is satisfied for Eq. (19), and solitary waves are formed in the dimer. Moreover, the analytical expression (19) compares favorably with the direct numerical solution of problem (15) that satisfies Eq. (14). Hence, the WKB approximation (19) can be regarded as an *ad hoc* analytical approximation of the solitary wave over the semi-infinite interval $\tau \in [0, +\infty)$. This is demonstrated in Fig. 9, where the numerical solution of Eq. (15) for $\varepsilon_n = 0.062\,913$ and the analytical solution (19) for $\varepsilon_n = 0.062\,748$ are compared. We note that the solutions are in agreement, especially in the finite interval of rapid oscillations of the response where the WKB approximation is valid.

In Table I we give the comparison of the set of discrete values $\{\varepsilon_n\}$ where solitary waves are realized in the dimer, computed in two different ways: (i) by direct numerical simulations of the normalized system (3b)—exact results in the right column; and (ii) by the numerical solutions of the

TABLE I. Parameter values ε_n for realization of solitary waves in the dimer.

n	Numerical simulation of the $O(\varepsilon)$ fast dynamics [Eq. (11)] ε_n	Numerical simulation of system (3b) ε_n
2	0.82835	
3	0.278115	0.3428
4	0.146747	0.1548
5	0.091702	0.0901
6	0.062913	0.0615
7	0.0458955	0.04537
8	0.034984	0.03448
16	0.0086818	0.00868

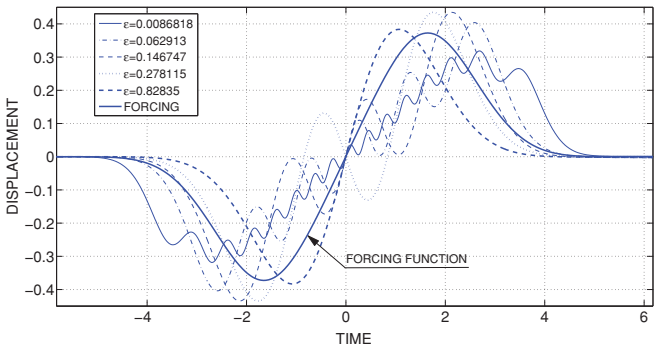

FIG. 10. (Color online) Numerical solutions of the fast dynamics [Eq. (11)] for certain values of ε_n at which solitary waves are realized in the dimer.

asymptotic model (11) [or equivalently Eq. (15)] describing the fast dynamics of the light beads—approximate results in the left column. As stated previously the results predicted by the asymptotic model (11) have physical meaning only for sufficiently small values of ε, so we expect better convergence of the two sets of results for decreasing values of ε_n (or for increasing order n). This is confirmed in the results listed in Table I, where we note that the error between the exact and approximate estimates decreases with increasing order n. Even though the asymptotic analysis predicts the existence of a solitary wave for $\varepsilon_2 = 0.828\,35$ (for $n = 2$), this is not confirmed by the exact numerical analysis. The reason for the absence of a solitary wave for $n = 2$ will be discussed below, and here we only make the remark that for this relatively large value of normalized mass ratio the slow-fast partition of the dynamics is not valid for describing the solitary wave in the dimer, so the asymptotic analysis is not expected to be valid in that range of values of ε.

We conclude this analysis by commenting that the antisymmetry conditions formulated for the solitary wave in the dimer may also be viewed in the context of imposing antiresonance conditions in the bead dynamics. In fact, the absence of a tail in the solitary wave is due to the antisymmetry conditions (13) and (14), resulting in an *antiresonance condition* in the dynamics of the dimer. This contrasts to a *resonance condition* in the dimer dynamics, which occurs when a phase difference of $\pi/2$ exists at $t = 0$ between the response $x_{(2p)1}(\tau)$ and the (slow) excitation $f_{2p}(\tau)/\varepsilon$ of the fast oscillator [Eq. (15)]. Current research by the authors indicates that such a nonlinear resonance leads to the drastic reduction of the transmitted normalized force in the plot of Fig. 8(a) for $\varepsilon \approx 0.59$, through the magnification of the amplitudes of the traveling waves in the tail of the propagating pulse and corresponding maximum radiation of a significant part of the energy of the pulse as it scatters at the interfaces between heavy and light beads; we note that this is the exact opposite of the "zero tail" situation of the solitary wave corresponding to the condition of antiresonance.

In this context, the formation of the solitary wave in the dimer for the eigenvalue $\varepsilon = \varepsilon_n$ determines the order of antiresonance satisfied by the velocity profile of the solitary wave. Because the characteristic frequency $\Omega_{2p}(\tau)$ of the linearized system (15) is slowly varying, we must resort to a nonstandard definition of antiresonance in this case. Hence, we will refer to the number of peaks exhibited in the fast oscillations of a light bead compared to the two peaks of the applied force $f_{2p}(\tau)$ [cf. Fig. 10 where numerical solitary waves of the asymptotic model (11) or (14) are depicted]. Considering the first value $\varepsilon = \varepsilon_2$ predicted by the asymptotic model (11), we note that the fast oscillations of the light bead also possess two peaks, so this would correspond to a condition of 1 : 1 antiresonance between the applied force and the light bead response; however, as discussed previously this value of ε does not correspond to a physically realizable solitary wave. Proceeding to the next eigenvalue $\varepsilon = \varepsilon_3$ the fast oscillation response of the light bead possesses four peaks (cf. Fig. 10), so this would be a condition of 1 : 2 antiresonance, which indeed corresponds to a class of physically realizable solitary waves parametrized by energy. Extending this argument, the class of solitary waves corresponding to the eigenvalue $\varepsilon = \varepsilon_n$ corresponds to a $1 : (n-1)$ antiresonance, with the fast oscillation response of the light bead possessing $2n$ peaks compared to the two peaks of the forcing function $f_{2p}(\tau)$. Hence, as the order n increases (and the eigenvalue ε_n decreases), the fast frequency of the light bead response also increases. It follows that each solitary wave solution in the dimer corresponds to a precise antiresonance condition, which is equivalent to the antisymmetry conditions posed previously.

Again, we emphasize that the asymptotic analysis is valid only as long as the slow-fast time scale separation exists. Therefore, we do not expect that the asymptotically predicted value of $\varepsilon_2 = 0.829$ will correspond to the formation of a solitary wave in the dimer, because that would imply an exact 1:1 antiresonance between the slow and fast dynamics, a fact that contradicts the slow-fast time scale partition upon which the asymptotic analysis is based. However, the rest of the asymptotically predicted antiresonance conditions do correspond to physically realizable solitary waves in the dimer starting from $\varepsilon_3 = 0.2781$, which corresponds to (1 : 2) antiresonance between the slow and fast dynamics and indeed was numerically detected in the dimer chain (see Fig. 4).

Finally, we note that the lack of a uniformly valid analytical approximation for system (15) [for given slow frequency $\Omega_{2p}(\tau)$ and forcing $f(\tau)$] prevents us from stating that there is a countable infinity of families of solitary waves that can be realized in a typical elastic dimer system. The fact that the derived WKB solution (19) is valid only in finite intervals $\tau \in [0, T^*]$, $T^* < +\infty$, prevents us from formulating a boundary

value problem by imposing conditions of decay of the motion at infinity. Hence, we can only conjecture on the existence of a countable infinity of families of solitary waves in the dimer.

IV. CONCLUDING REMARKS

Summarizing the findings of this work, we demonstrated the existence of a new family of solitary waves in one-dimensional granular dimer chains with elastic interactions between beads according to the Hertzian interaction law and in the absence of precompression. The problem was brought in normalized form, and ultimately was governed by a single parameter ε, defined as the ratio of normalized masses between the light and heavy beads of the dimer. Hence, our results are applicable to a general class of dimers of different materials and geometric properties.

The solitary waves in the dimer reported in this work can be considered to be analogous to the solitary wave of the homogeneous granular chain studied by Nesterenko [1], in the sense that these localized solitary pulses do not involve separations between beads; rather they satisfy special anti-symmetries, or equivalently antiresonances in the dynamics. We may conjecture, therefore, that these solitary waves are the direct products of a countable infinity of antiresonances in the dimer. Moreover, we found that the solitary waves in the dimer propagate faster than the solitary wave in the homogeneous granular chain obtained in the limit of no mass mismatch and composed of only heavy beads. This finding, which might seem to be counterintuitive, indicates that under certain conditions nonlinear antiresonances can increase the speed of disturbance propagation in periodic granular media, by providing different ways of transferring energy to the far field of these media. From a practical point of view, this result can have interesting implications in applications where granular media are employed as shock transmitters or attenuators.

The asymptotic analysis of this work was based on slow-fast partition of the dynamics, and can be applied to a more general class of granular media with periodic or nonperiodic disorders. Such studies would identify efficient nonlinear mechanisms for effectively propagating energy through periodic granular media. An additional interesting topic of application of the presented methodologies is to employ resonances for the reverse scope of efficiently attenuating propagating pulses in granular media.

ACKNOWLEDGMENTS

This work was funded by MURI Grant No. US ARO W911NF-09-1-0436; Dr. David Stepp is the grant monitor. The authors are grateful to Professor O.V. Gendelman of Technion and to Dr. Lukas Pichler and Mohammed Hasan Arif of the University of Illinois at Urbana-Champaign for fruitful discussions and suggestions. The comments of the reviewers were particularly helpful in the revision of our manuscript.

[1] V. F. Nesterenko, *Dynamics of Heterogeneous Materials* (Springer, New York, 2001).
[2] S. Sen *et al*., Phys. Rep. **462**, 21 (2008).
[3] A. Chatterjee, Phys. Rev. E **59**, 5912 (1999).
[4] A. Molinari and C. Daraio, Phys. Rev. E **80**, 056602 (2009).
[5] C. Coste *et al*., Phys. Rev. E **56**, 6104 (1997).
[6] A. C. Scott *et al*., Proc. IEEE **61**, 1443 (1973).
[7] E. B. Herbold *et al*., Acta Mech. **205**, 85 (2009).
[8] M. A. Porter *et al*., Physica D **238**, 666 (2009).
[9] N. Boechler *et al*., Phys. Rev. Lett. **104**, 244302 (2010).
[10] G. Theocharis *et al*., e-print arXiv:1009.0885v1.
[11] M. A. Porter *et al*., Phys. Rev. E **77**, 015601(R) (2008).
[12] Y. Starosvestky and A. F. Vakakis, Phys. Rev. E **82**, 026603 (2010).
[13] A. F. Vakakis *et al*., *Normal Modes and Localization in Nonlinear Systems* (Wiley, New York, 1996).
[14] U. Harbola *et al*., Phys. Rev. E **82**, 011306 (2010).
[15] S. Sen and M. Manciu, Phys. Rev. E **64**, 056605 (2001).
[16] C. M. Bender and S. A. Orszag, *Advanced Mathematical Methods for Scientists and Engineers: Asymptotic Methods and Perturbation Theory* (Springer, New York, 1991).